Ultrastructural Morphology of *Uromyces transversalis* Infection of Resistant and Susceptible Gladiolus Hosts and a Nonhost, *Zea mays*

J. F. Ferreira and F. H. J. Rijkenberg

Plant pathologist, Fynbos Research, Vegetable and Ornamental Plant Research Institute, Private Bag, Elsenburg 7607; and professor, Department of Microbiology/Plant Pathology, University of Natal, P.O. Box 375, Pietermaritzburg 3200, Republic of South Africa.

Part of a Ph.D. dissertation submitted to the University of Natal.

We gratefully acknowledge the funding by the Department of Agricultural Development and technical assistance of Electron Microscope Units at the University of Natal, University of Pretoria, and Plant Protection Research Institute, Rietondale. We thank B. H. Boelema and K. Mendgen for their critical review of the manuscript and M. G. Wright for the statistical analysis.

Accepted for publication 10 September 1990 (submitted for electronic processing).

ABSTRACT

Ferreira, J. F., and Rijkenberg, F. H. J. 1991. Ultrastructural morphology of *Uromyces transversalis* infection of resistant and susceptible gladiolus hosts and a nonhost, *Zea mays*. Phytopathology 81:596-602.

The infection structures of gladiolus rust, *Uromyces transversalis*, on and in host leaves of the susceptible gladiolus cultivar (Goldfield) and resistant species (*Gladiolus daleni*) and in leaves of the nonhost (*Zea mays*) were examined by scanning and transmission electron microscopy. The number of germinated urediospores that formed appressoria on the resistant host was significantly fewer than the number formed on the susceptible host. The major determinant of resistance in the host was manifested in the significant proportion of substomatal vesicles with primary hyphae that aborted before the formation of haustorial mother cells and/or secondary hyphae. This was correlated with a similar reaction in the nonhost. The abortion was attributed to the putatively incomplete adhesion of haustorial mother cells to mesophyll cells. In the nonhost, although no secondary hyphae were formed, some haustorial mother cells were formed, and a significant proportion of primary hyphae did not form haustorial mother cells and/or secondary hyphae.

The host range of *Uromyces transversalis* (Thüm.) Winter includes the following genera: *Gladiolus* L., *Tritonia* L., *Watsonia* L. (4), *Crocosmia* L. (2,15), and *Freesia* L. (14). In a previous study (6), gladiolus cultivars, species, and breeding lines were evaluated for resistance to the gladiolus rust pathogen, *U. transversalis*, and results indicated resistance in *G. daleni* Hill. & Burtt (syn. = *G. natalensis*) ecotypes. *G. daleni* therefore appeared to be a good candidate for an investigation into the morphology of a resistance mechanism against gladiolus rust.

In the past, quantitative studies on the morphology of rust infection structures in susceptible and resistant hosts and nonhosts have been done successfully with the aid of light (7–9,11,16,17) and fluorescence (19–21) microscopy.

Light microscopy showed that *Puccinia graminis* infection of a nonhost, corn, was halted after appressorium development and, in one case, before haustorium mother cell formation (16). Extensive fluorescence microscopy by Niks (19,20) quantitatively demonstrated the early arrest of *P. hordei* and *P. recondita tritici* infection of barley and wheat immediately after the formation of the first haustorium mother cells. Of particular interest was the partially resistant infection of *P. hordei*, which aborted after the formation of the first infection hyphae (20). Ferreira demonstrated in preliminary trials that the use of light and fluorescence microscopy for the investigation of gladiolus resistance was prohibited by the extraordinary thickness of gladiolus leaves (*unpublished data*). Because electron microscopy has been used previously to highlight certain aspects of infection structures in resistant or susceptible tissue (18), we decided to investigate the development of infection structures of *U. transversalis* in a unique quantitative manner with the aid of scanning and transmission electron microscopy. This was done on and in the leaves of a susceptible gladiolus cultivar (Goldfield), a resistant species (*G. daleni*) and a nonhost (*Zea mays* L.). The aim of the study was to determine the morphological expression of the resistance mechanism involved in gladiolus rust and how it compares with that of the nonhost.

MATERIALS AND METHODS

The terminology used by Littlefield and Heath (18) is followed throughout unless otherwise indicated.

Rust propagation and inoculation. Freshly harvested urediospores of *U. transversalis* (PREM 47693, National Collection of Fungi, Plant Protection Research Institute, Pretoria) produced on 2-mo-old susceptible Goldfield grown in a glasshouse (18–35 C) were used to inoculate host and nonhost plants. For inoculation, spores were brushed over one surface of the distal third of mature hosts of the cultivar, species, and a nonhost, corn. The unifacial, tangential leaves of gladiolus preclude distinction between an abaxial and adaxial surface; on corn leaves the adaxial surface was inoculated. Inoculated plants were placed in a dew chamber at 20 C for 16 h in the dark and then moved to the glasshouse (18–35 C). The experiment was conducted twice with each of two cultivars, two species, and two corn plants.

Scanning electron microscopy. Four pieces per leaf from two leaves of two plants of the cultivar, species, and nonhost were excised at 96 h postinoculation (hPI). The pieces were cut into rectangles of 2 × 4 mm and fixed in 3% glutaraldehyde in a 0.05 M sodium cacodylate buffer, pH 6.8–7.2, for 12 h or overnight, washed twice in buffer, postfixed for 3 h in 2% osmium tetroxide in buffer, washed twice in buffer, and dehydrated in a graded ethanol series. Samples were then critical-point dried with carbon dioxide as a transition fluid and mounted on copper stubs. The epidermis of the gladiolus leaf samples were removed manually under a stereomicroscope, and corn leaf epidermis was removed with the stub method as described earlier (5). The stripped epidermis and the tissue from which the epidermis was stripped were gold coated in a Balzers sputter coater and examined with a JEOL JSM-35 scanning electron microscope operated at 15 kV.

Data presentation. Total numbers of infection structures on and in leaf pieces of the species and the cultivar were determined by scanning electron microscopy. The data obtained from the leaf surface were processed separately from data originating from inside the leaf because the stripping method precludes the stripping of the entire specimen, and therefore the fate of not all appressoria could be determined. On the leaf surface, the total number of

germinated urediospores with appressoria was expressed as a percentage of the germinated urediospores without appressoria. The data were analyzed using a 2 × 2 contingency table with Yates correction for continuity to determine whether there was a significant difference in the proportion of appressoria formed in the susceptible and resistant host. Inside the leaf, infection structure development was categorized (5) into: substomatal vesicles (SSVs), SSVs with primary hyphae before formation of the haustorial mother cell (HMC), SSVs with HMCs and/or secondary hyphae on the stripped epidermis, and SSVs with intercellular hyphae, an infection so well advanced that stripping of the epidermis fails to dislodge the accumulated structures from the underlying tissue. Because the attainment of the final developmental stage implies that the other three stages have been successfully completed, totals presented under each category are cumulative. A 2 × 4 contingency table was used to test whether the proportions of infection structures were dependent on susceptibility or resistance. The 2 × 4 contingency table was reduced to a 2 × 2 contingency table to determine whether there is a difference between the proportion of secondary hyphae that would be formed in the susceptible and resistant hosts. Finally a goodness of fit was used to determine whether all primary hyphae formed secondary hyphae in the resistant host, or if the resultant proportion of secondary hyphae formed deviated significantly from the proportion expected to form. These cumulative values then were represented schematically as a percentage of the total infection structures in the leaf interior. In the nonhost, a goodness of fit test was conducted to determine whether all primary hyphae developed into secondary hyphae, or if the resultant proportion of secondary hyphae formed deviated significantly from the proportion expected to form.

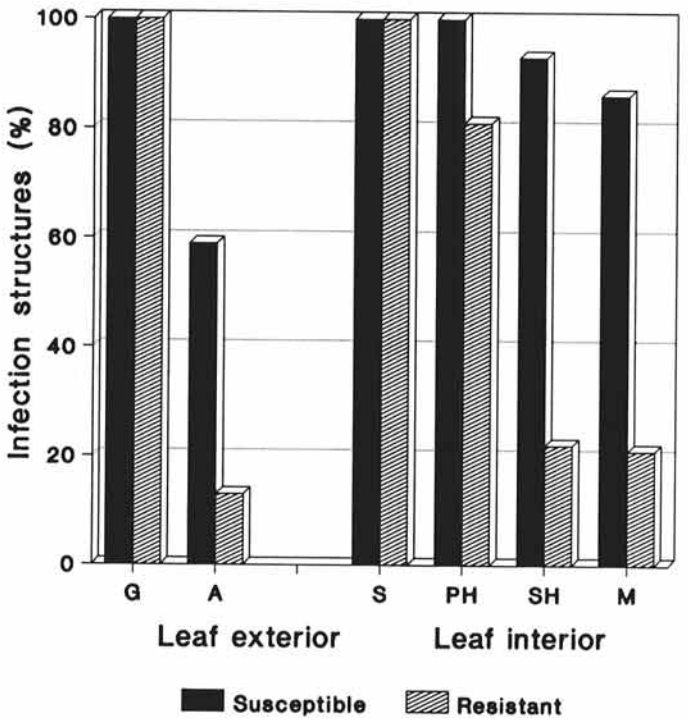

Fig. 1. Developmental stages of infection structures of *Uromyces transversalis* interrupted at 96 h postinoculation on and in leaves of a susceptible gladiolus cultivar (Goldfield) and a resistant gladiolus species (*Gladiolus daleni*) examined by scanning electron microscopy. The results are divided into infection structures on the leaf surface and inside the leaf. Germinated urediospores that did form appressoria (A) on the resistant or susceptible host leaves are expressed as a percentage of germinated urediospores (G) regardless of appressorium formation. The infection structures are categorized into SSV (S), SSV with primary hyphae including the initials until before haustorial mother cell formation (PH), SSV with haustorial mother cell and/or secondary hyphae (SH), and SSV with intercellular hyphae (M). These categories are expressed as a percentage of all the structures in the resistant and susceptible hosts.

Transmission electron microscopy. Leaves (96 hPI) of the cultivar and the species, inoculated and uninoculated, were cut into rectangles of 2 × 4 mm and fixed overnight under 200 mm Hg vacuum in 3% glutaraldehyde in a 0.05 M sodium cacodylate buffer (pH 6.8–7.2), washed twice in buffer, and postfixed in 2% osmiun tetroxide in the same buffer. Dehydration was performed either in an ethanol series for embedding in Spurr's resin (23) or in an acetone series followed by two changes in propylene oxide leading to embedding in Epon/Araldite (1) resin. The specimen blocks were sectioned (50–70 nm) with glass knives and sections were stained according to the method of Reynolds (22) and viewed with a JEOL 100 C or CX transmission electron microscope operated at 60 and 80 kV, respectively.

RESULTS

Percentages of observed infection structures on and in the leaf pieces of the cultivar and species are presented in Figure 1. A total area of 25.53, 35.42, and 38.25 mm^2 was observed for the susceptible host, resistant host, and nonhost, respectively. The development of the fungus was arrested at 96 hPI, and because the fate of not all appressoria could be determined, the results for pre- and postpenetration are evaluated separately.

Prepenetration events. On the leaf surface of the cultivar, 96 hPI, the percentage (Fig. 1) of germ tubes that successfully located stomata and formed appressoria (Figs. 2 and 3) appeared much higher than on the leaf surface of *G. daleni*. Contingency table analysis of results (Table 1) show that there is a highly significant difference in proportion of appressoria formed on the susceptible and resistant host plants. The infection peg formed by an appressorium over a stoma of the species was occasionally (5%) bifurcate (Fig. 4). Germ tubes often failed to locate stomata (Fig. 5). No evidence for directional growth of germ tubes towards stomata was found on either of the hosts, and germ tubes grew more often over stomata without forming appressoria on resistant than on susceptible leaves (Table 1). The trichomes on the susceptible leaf surface (Fig. 6) were half the height of those on the resistant leaf surface (Fig. 7) measured in serial section with light microscopy. In other respects the leaf surface morphology was similar. The germ tubes were often aerial (Fig. 7) on both hosts.

Prehaustorial events. In Figure 1, the infection structures are categorized into SSV (S); SSV with primary hyphae (denoted as infection hyphae by Littlefield and Heath [18], here used as primary and secondary hyphae according to Hughes and Rijkenberg [13]) including the initials until before HMC formation (PH); SSV with HMC (Fig. 8) and/or secondary hyphae (SH); and SSV with intercellular hyphae (M). An analysis (Table 2) of the total number of observed categorized infection structures

TABLE 1. Scanning electron microscope observations on the development of germinated urediospores of *Uromyces transversalis* on susceptible and resistant gladiolus leaves[a]

	Susceptible[b]		Resistant[b]			
Replicate	G + A	G − A	G + A	G − A	χ^2	P[c]
1	63	56	36	282	83.2	*
2	48	38	43	233	54.3	*
3	39	20	39	313	95.9	*
4	74	48	56	275	81.2	*
5	59	36	64	431	113.8	*
Total	283	198	238	1,534	436.2	**

[a] Results of 2 × 2 contingency table analysis with Yates correction for continuity are presented. The null hypothesis that no difference in proportion of appressoria was formed on susceptible and resistant plants was tested.

[b] G + A = germinated urediospores terminated in an appressorium over a stoma; G − A = germinated urediospores which did not terminate in an appressorium.

[c] One asterisk indicates $P < 0.01$ and two asterisks indicate $P < 0.001$ with df = 1 in all replicates.

inside the leaf showed proportional differences highly dependent ($P < 0.001$) on susceptiblility or resistance. On the basis of this result, a further analysis conducted showed a highly significant ($P < 0.001$) difference in the proportion of secondary hyphae that formed in the susceptible and resistant host (Table 3). A goodness of fit test (Table 4) showed that a significantly ($P < 0.001$) lower proportion of primary hyphae did not form secondary hyphae (Fig. 9) and/or HMCs in the resistant host than the null hypothesis proposed. The schematic representation of this data (Fig. 1) shows the difference in percentage of structures formed. At 96 hPI, 86% (Fig. 1) of the infection structures inside the susceptible leaf tissue had developed into the final observed stage

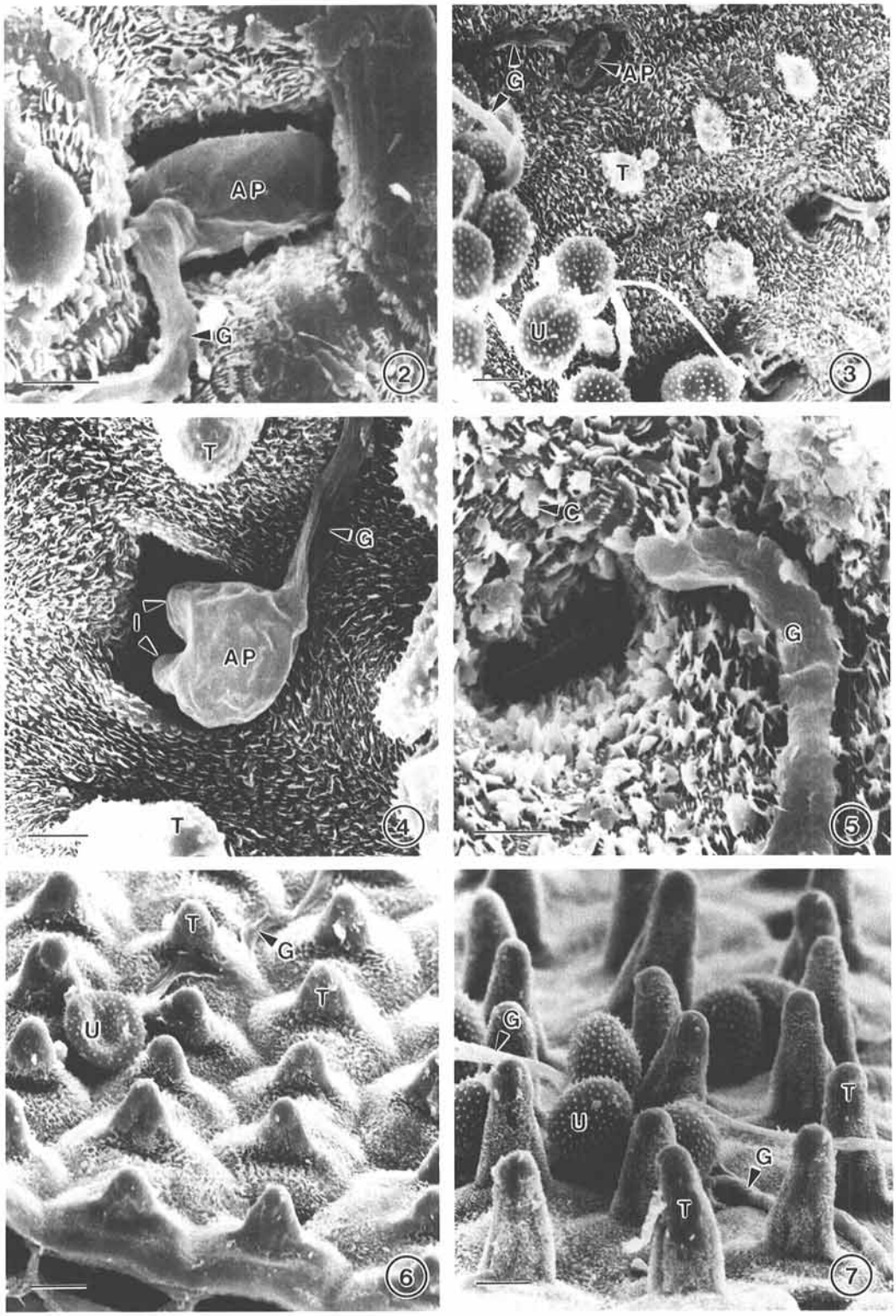

Figs. 2–7. Scanning electron micrographs of infection structures of *Uromyces transversalis*, 96 h postinoculation, on the leaf surfaces of unstripped samples of a susceptible gladiolus cultivar (Goldfield) (2, 3, and 6) and a resistant gladiolus species (*Gladiolus daleni*) (4, 5, and 7). AP = appressorium; C = cuticle; G = germ tube; I = infection peg; T = trichome; U = urediospore. **2,** Normal development of germ tube into appressorium located in prestomatal chamber of leaf. **3,** Urediospores and germ tubes that have developed into appressoria on leaf surface with trichomes. **4,** Germ tube with appressorium over stoma between two trichomes. Appressorium has bifurcate infection peg. **5,** Germ tube that has failed to locate stoma on cuticle. **6,** Urediospore with surface-adherent germ tube between trichomes. **7,** Urediospores and aerial and surface-adherent germ tubes between trichomes. Bars = 10 μm.

(Fig. 10). In the resistant tissue, 21% of the infection structures had developed into the final stage (Fig. 1). Concomitantly, a higher percentage of prehaustorial mother cell SSVs was observed in the resistant tissue (Fig. 1). The SSVs in the resistant host appeared normal, but their development had been arrested. Besides the normal infection structures, which were swollen and showed no signs of structural disorganization, there were aborted infection structures, which were structurally disorganized and showed signs of collapse. Ten percent of the infection structures in the resistant host aborted at the final development stage (Fig. 11). The primary hyphae of gladiolus rust infection structures in the cultivar, after delimiting an HMC, would adhere to mesophyll cells and sever

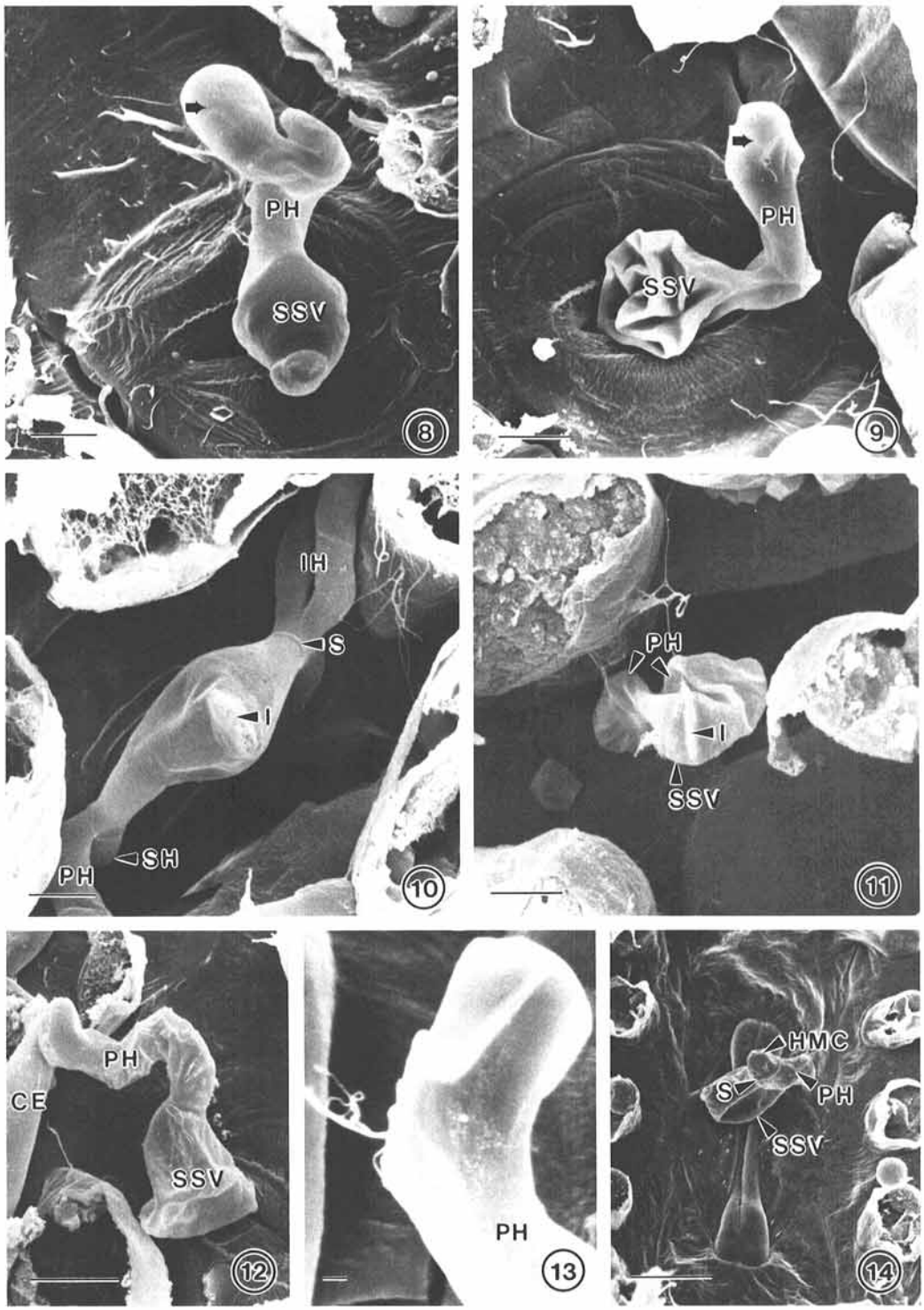

Figs. 8–14. Comparative scanning electron micrographs of the early infection structures of *Uromyces transversalis* 96 h postinoculation inside the leaves of stripped samples of a susceptible cultivar (Goldfield) (8 and 10), resistant species (*Gladiolus daleni*) (9, 11–13), and a nonhost (*Zea mays*) (14). CE = mesophyll cell; HMC = haustorial mother cell; I = interconnective tube; IH = intercellular hyphae; PH = primary hypha; S = septum; SH = secondary hypha; SSV = substomatal vesicle. **8,** Substomatal vesicle and primary hypha with swollen tip (arrow) developed on inside of stoma. **9,** Collapsed substomatal vesicle and primary hypha with swollen tip (arrow) on inside of stoma. **10,** Mature substomatal vesicle with scar of interconnective tube. In substomatal chamber, septum delimits intercellular hyphae on one side of the substomatal vesicle and primary and secondary hyphae on the other. **11,** Collapsed substomatal vesicle with scar of interconnective tube and collapsed primary hyphae. **12,** Collapsed substomatal vesicle and primary hypha in contact with mesophyll cell showing swollen nature of hyphal tip. **13,** Close-up of primary hypha after undamaged tip has separated from mesophyll cell during stripping. **14,** Collapsed substomatal vesicle and primary hypha after formation of haustorial mother cell, indicated by septum, on inside of corn stoma. 8–11, bar = 5 μm. 12–14, bar = 10 μm.

at, or close to, the SSV during epidermis stripping.

In the resistant host, primary hyphae of SSVs aborted (Figs. 11–13) after establishing loose contact (Fig. 12) with the mesophyll cell. Tips of such primary hyphae failed to delimit an HMC as shown by the absence of an HMC septum and separated from the cell wall (Figs. 9, 12, and 13) during stripping of the epidermis. The tips of these primary hyphae often retained their shape at 96 hPI, whereas their SSVs normally collapsed (Fig. 9). In the susceptible reaction, the primary hyphae developed asynchronously (Fig. 8), whereas in the resistance reaction, the primary hypha opposite the first-developed primary hypha failed to develop on the often collapsed SSV (Figs. 9 and 12). Infection structures of *U. transversalis* that did develop on the stripped epidermis of the nonhost, corn, aborted soon after the formation of the HMC septum (Fig. 14). A goodness of fit test (Table 5) showed that a significant ($P < 0.05$) proportion of primary hyphae did not develop into secondary hyphae in the nonhost. The tip of the aborted primary hypha appeared electron dense in section in the resistant leaf tissue (Fig. 15).

Adherence at the HMC-mesophyll cell interface, after haustorial neck formation in the resistant host, was apparently partial, and less of the adhesive material was evident. In those instances, the connection between the HMC and the mesophyll cell occasionally was severed during specimen preparation (Fig. 16). This interface in the susceptible interaction was never observed to sever. Intercellular hyphae were more abundant in the cultivar than in the species. Hyphae in the intercellular spaces of the cultivar were always in close contact with the host cells or one another (Fig. 17). A highly osmiophilic material, which we interpret to be of an adhesive nature, was found between such hyphae and between hyphae and mesophyll cells (Fig. 17). In the resistance reaction, the hyphae normally were not in close contact with either the mesophyll cells or one another. Where adhesion to a mesophyll cell or to other hyphae did occur, the adhesive material at the interface was less osmiophilic than in the susceptible reaction (Figs. 18–20). Less osmiophilic adhesive also was demonstrated where an HMC did form and penetrate the mesophyll cell wall (Fig. 21).

TABLE 2. Scanning electron microscope observations on the proportions of developmental stages of infection structures in susceptible and resistant gladiolus leaves[a]

	Infection structures[b]				
	S	PH	SH	M	Total
Susceptible	168	168	159	145	640
Resistant	114	92	25	24	255
Total	282	260	184	169	895

$\chi^2 = 62.7$; df = 3; $P < 0.001$

[a] A 2 × 4 contingency table was used to test the null hypothesis that the development of the various structures inside the leaf was independent of susceptibility or resistance of host.

[b] Infection structures are formed sequentially in the following order; S = substomatal vesicle, PH = primary hyphae, SH = secondary hyphae, M = substomatal vesicle with intercellular hyphae.

TABLE 3. Scanning electron microscope observations on the development of primary hyphae of *Uromyces transversalis* into secondary hyphae in susceptible and resistant gladiolus leaves[a]

	Susceptible[b]		Resistant[b]			
Replicate	p + S	p − S	p + S	p − S	χ^2	P[c]
1	29	3	1	8	18.8	*
2	31	1	5	19	31.3	*
3	30	0	6	18	30.5	*
4	31	2	6	15	22.4	*
5	38	3	7	7	10.1	*
Total	159	9	25	67	127.6	**

[a] Results of 2 × 2 contingency table analysis with Yates correction for continuity are presented. Inspection of data presented in Table 2 suggested that the significant χ^2 was calculated largely due to column 3 of the table. On the basis of this, the null hypothesis that no difference in proportion of secondary hyphae was formed in susceptible and resistant hosts was tested.

[b] p + S = primary hyphae (p) that did develop into secondary hyphae (S); p − S = primary hyphae that did not develop into secondary hyphae or beyond it.

[c] One asterisk indicates $P < 0.01$ and two asterisks indicate $P < 0.001$ with df = 1 in all replicates.

DISCUSSION

Although the gladiolus is a monocotyledonous plant and rust germ tubes on the leaves of several monocotyledonous plants are directional (12,18), no directional growth was observed in this study and, therefore, could not be responsible for the higher percentage of appressoria formed on the susceptible cultivar. On the surfaces of both the cultivar and the species, germ tubes often grew over stomata, failing to recognize them, but the failure frequency on the leaf surface of the resistant host was significantly higher. The aborted appressoria over the stomata of the resistant host often had an infection peg morphology different from that described by Ferreira and Rijkenberg (5) for *U. transversalis*. The bifurcate peg of the appressorium morphologically resembled that described by Hughes and Rijkenberg (13) for *P. sorghi* Schw. on corn. No abortion of appressoria similar to the resistant reaction was observed by scanning electron microscopy on the susceptible leaf surface.

Leath and Rowell (16) demonstrated that infection structures of *P. graminis* in a nonhost, corn, were halted after the formation of appressoria and, with one exception, before the formation of HMCs. In a comparative study on nonhost interactions of other rust fungi, it was shown that nonhosts do induce the formation of HMC septa (10). A similar result was found in the present study where, although a significant number of primary hyphae did not develop HMCs and/or secondary hyphae, quite a high proportion did if the nonhost, corn, is compared with the results obtained with the resistant host. In an extensive study, Niks (19,20) demonstrated with fluorescence microscopy that *P. hordei* and *P. r. tritici* infection of wheat and barley cultivars were arrested early, immediately after the formation of the first HMCs (19). *P. hordei*, in particular, aborted after the formation of the first infection hyphae, probably primary hyphae according to definition (13), and few HMCs (20). The present study, however,

TABLE 4. Scanning electron microscope observations on the development of the primary hyphae into secondary hyphae in gladiolus leaves resistant to *Uromyces transversalis*[a]

	Observed	Expected
Primary hyphae	124	124
Secondary hyphae	43	124

[a] The data presented in Table 3 suggested that the significant χ^2 is largely due to the data on the resistant leaves at secondary hypha formation. A goodness of fit test was used to determine if the resultant proportion of secondary hyphae formed deviated significantly from the proportion expected to form. $\chi^2 = 52.9$; df = 1; $P < 0.001$.

TABLE 5. Scanning electron microscope observations on the development of the primary hyphae into secondary hyphae in corn leaves, a nonhost to *Uromyces transversalis*[a]

	Observed	Expected
Primary hyphae	19	19
Secondary hyphae	9	19

[a] A goodness of fit test was used to determine if the resultant proportion of secondary hyphae formed deviated significantly from the proportion expected to form. $\chi^2 = 5.26$; df = 1; $P < 0.05$.

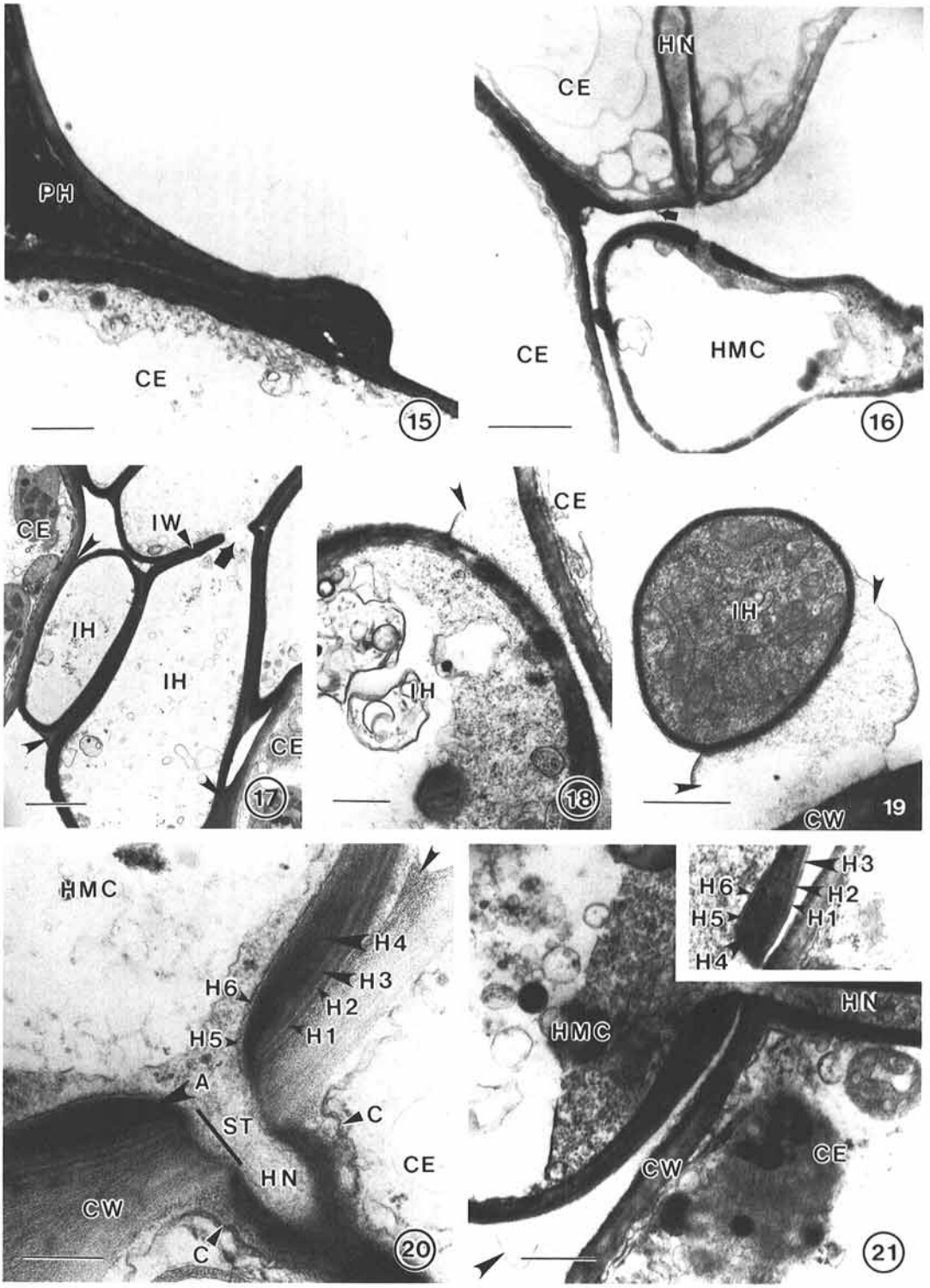

Figs. 15–21. Transmission electron micrographs of intercellular hyphae and haustorial mother cells of *Uromyces transversalis* in leaves of a susceptible cultivar (Goldfield) (17 and 20) and a resistant species (*Gladiolus daleni*) (15, 16, 18, 19, and 21). A = annulus part of the interwall penetration torus; C = collar; CE = mesophyll cell; SW = mesophyll cell wall; HMC = haustorial mother cell; HN = haustorial neck; H1–H6 = haustorial mother cell wall layers close to the penetration site; IH = intercellular hypha; IW = infolded wall; ST = stem part of the intrawall penetration torus. **15,** Section of aborted primary hypha in contact with mesophyll cell, 24 h postinoculation. **16,** Section of haustorial mother cell severed from mesophyll cell at penetration site. Remnants (arrow) of adhesive layer are visible close to haustorial neck. **17,** Section through intercellular hyphae between mesophyll cells showing their close contact and osmiophilic material (small arrows) at their interfaces. Intercellular hypha with infolded wall. The opening is partially occluded by vesicle (large arrow). **18,** Section through intercellular hypha closely associated with mesophyll cell with little osmiophilic material (arrow). **19,** Section through intercellular hypha attached to mesophyll cell wall with little osmiophilic material (arrows) at hypha-mesophyll cell interface. **20,** Oblique section through haustorial mother cell close to penetration site showing intrawall penetration site which consists of annulus and stem and haustorial neck with collar on either side. Evident in the micrograph are six layers in haustorial mother cell wall (H1–H6) and osmiophilic material (arrow) at haustorial mother cell and host cell interface in susceptible reaction. **21,** Section through haustorial mother cell and haustorial neck at penetration site showing less osmiophilic material (arrow) at interface with mesophyll cell. 18 and 21, bar = 0.5 μm. 15 and 19, bar = 1 μm. 16, 17, and 20, bar = 2 μm.

has shown that scanning electron microscopy data can be used quantitatively where conventional methods are inadequate due to, for example, thickness of gladiolus leaves. We have demonstrated that resistance to gladiolus rust is manifested in the loose adhesion of *U. transversalis* primary hyphae, HMCs, and intercellular hyphae to the mesophyll cells of the species. Epidermis stripping resulted in the tip of the primary hypha separating from the mesophyll cell of the species, whereas in the susceptible reaction, stripping resulted in the severance of the primary hypha at, or close to, the SSV. The tip of the primary hypha in the cultivar had developed into an HMC and adhered tightly to the mesophyll cell of the cultivar.

Light and electron microscope studies (9) on *Vicia faba* and *U. phaseoli* var. *vignae* showed that adherence of the HMC to the cell wall inhibited haustorium formation. Loose adhesion, similar to that at the HMC-mesophyll cell interface, also was exhibited in the resistance reaction among intercellular hyphae. The fact that a haustorial apparatus occasionally formed, although the adhesion was loose, suggests that tight adhesion between fungus and cell is not always a prerequisite for penetration. It seems likely that, where an HMC is wedged tightly between two host cells, the presence of an efficient adhesive layer is of lesser importance. Chong et al (3) showed that the outermost layer of the HMC of *P. graminis* f. sp. *tritici* is composed of glycoprotein-containing α-linked glucose and/or mannose, glycoprotein-containing sugars with vicinal OH groups and unsaturated lipid (possibly lipoprotein). It is possible that these molecules may play a role in fungus-host cell contact and in the process of recognition or nonrecognition between host cells and fungal infection hyphae.

LITERATURE CITED

1. Anderson, W. A., and André, J. 1969. The extraction of some cell components with pronase and pepsin from thin sections of tissue embedded in an Epon-Araldite mixture. J. Microsc. (Paris) 7:343.
2. Bisby, G. R., and Wiehe, P. O. 1953. The rusts of Nyassaland. The Commonwealth Mycological Institute, Kew. Mycological Papers 54:12.
3. Chong, J., Harder, D. E., and Rohringer, R. 1985. Cytochemical studies on *Puccinia graminis* f. sp. *tritici* in a compatible wheat host. I. Walls of intercellular hyphal cells and haustorium mother cells. Can. J. Bot. 63:1713-1724.
4. Doidge, E. M. 1950. The South African fungi and lichens to the end 1945. Bothalia 5:450.
5. Ferreira, J. F., and Rijkenberg, F. H. J. 1989. Development of infection structures of *Uromyces transversalis* in leaves of the host and a non-host. Can. J. Bot. 67:429-433.
6. Ferreira, J. F., Verryn, S., and Rijkenberg, F. H. J. 1990. The phenotypical responses of gladiolus germplasm with different degrees of resistance to *Uromyces transversalis*. Euphytica 49:215-221.
7. Heath, M. C. 1971. Haustorial sheath formation in cowpea leaves immune to rust infection. Phytopathology 61:383-388.
8. Heath, M. C. 1972. Ultrastructure of host and non-host reactions to cowpea rust. Phytopathology 62:27-38.
9. Heath, M. C. 1974. Light and electron microscope studies of the interactions of host and non-host plants with cowpea rust—*Uromyces phaseoli* var. *vignae*. Physiol. Plant Pathol. 4:403-414.
10. Heath, M. C. 1977. A comparative study of non-host interactions with rust fungi. Physiol. Plant Pathol. 10:73-88.
11. Hilu, H. M. 1965. Host-pathogen relationships of *Puccinia sorghi* in nearly isogenic resistant and susceptible seedling corn. Phytopathology 55:563-569.
12. Hoch, H. C., Staples, R. C., Whitehead, B., Comeau, J., and Wolf, E. D. 1987. Signaling for growth orientation and cell differentiation by surface topography in Uromyces. Nature (London) 235:1659-1662.
13. Hughes, F. L., and Rijkenberg, F. H. J. 1985. Scanning electron microscopy of early infection in the uredial stage of *Puccinia sorghi* in *Zea mays*. Plant Pathol. 34:61-68.
14. Jørstad, I. 1956. Re liquiae Lagerheimianae. African Uredinales. Arch. Bot. 2:563-598.
15. Kuiper, K., and Boerema, G. H. 1972. Quarantine aspects of the epidemiology of soil-borne pathogens. Eur. Mediterr. Plant Prot. Organ. (EPPO) Bull. 7:61-68.
16. Leath, K. T., and Rowell, J. B. 1966. Histological study of the resistance of *Zea mays* to *Puccinia graminis*. Phytopathology 56:1305-1309.
17. Littlefield, L. J. 1973. Histological evidence for diverse mechanisms of resistance to flax rust, *Melampsora lini* (Ehrenb.) Lev. Physiol. Plant Pathol. 3:241-247.
18. Littlefield, L. J., and Heath, M. C. 1979. Ultrastructure of Rust Fungi. Academic Press, New York.
19. Niks, R. E. 1983. Comparative histology of partial resistance and non-host reaction to leaf rust pathogens in barley and wheat seedlings. Phytopathology 73:60-64.
20. Niks, R. E. 1983. Haustorium formation by *Puccinia hordei* in leaves of hypersensitive, partially resistant, and non-host plant genotypes. Phytopathology 73:64-66.
21. Niks, R. E., and Kuiper, H. J. 1983. Histology of the relation between minor and major genes for resistance of barley to leaf rust. Phytopathology 73:55-59.
22. Reynolds, E. S. 1963. The use of lead citrate at high pH as an electron-opaque stain in electron microscopy. J. Cell Biol. 17:208-212.
23. Spurr, A. R. 1969. A low-viscosity epoxy resin embedding medium for electron microscopy. J. Ultrastruct. Res. 26:31-43.